Phys. Status Solidi B **254,** No. 8, 1600700 (2017) / **DOI** 10.1002/pssb.201600700

physica status solidi b
www.pss-b.com
basic solid state physics

Incorporation of germanium for n-type doping of cubic GaN

Michael Deppe*[,1], Jürgen W. Gerlach[2], Dirk Reuter[1], and Donat J. As[1]

[1] Department of Physics, University of Paderborn, Warburger Str. 100, 33098 Paderborn, Germany
[2] Leibniz Institute of Surface Modification, Permoserstr. 15, 04318 Leipzig, Germany

Received 24 October 2016, revised 30 January 2017, accepted 10 February 2017
Published online 1 March 2017

Keywords cubic GaN, doping, germanium

* Corresponding author: e-mail michael.deppe@uni-paderborn.de, Phone: +49 5251 60 5839, Fax: +49 5251 60 5843

We introduce germanium as an alternative to silicon for n-type doping of cubic gallium nitride. Layers with electron concentrations up to $3.7 \times 10^{20}\,cm^{-3}$ were grown by plasma-assisted molecular beam epitaxy on 3C-SiC substrates. Time-of-flight secondary ion mass spectrometry (TOF-SIMS) measurements were performed to verify the incorporation of Ge into our layers. The incorporation of Ge is in good agreement with the trend of the Ge vapour pressure curve. For the highest doped sample a drop of the incorporation efficiency is observed. A reduction of the growth rate is noticed for high Ge fluxes. Additionally, a sample comprising an alternating pattern of Ge-doped and not intentionally doped interlayers was grown. In the recorded TOF-SIMS depth profile we observe that in doped regions the Ge concentration increases along the growth direction. A gradually decreasing amount of Ge is incorporated into each overlying not intentionally doped interlayer. We suppose these observations are due to segregation effects and a resulting accumulation of Ge at the sample surface during growth.

1 Introduction The fabrication of many semiconductor devices requires a precise control of p- and n-type doping of the material. For n-type doping of wurtzite GaN most commonly Si is used. It is well known that incorporation of Si in wurtzite GaN leads to tensile strain [1], whereas it has recently been shown that this is not the case for incorporation of Ge, allowing the growth of highly doped layers with improved crystalline quality [2, 3]. Several groups have demonstrated that Ge is well-suited to achieve electron concentrations above $10^{20}\,cm^{-3}$ in high-quality films [4–6] as well as in advanced structures like nanowires [7].

Due to spontaneous and piezoelectric polarization fields in wurtzite GaN-based heterostructures, the performance of devices can be impaired. One approach to overcome these effects is to grow the metastable cubic zinc-blende phase of GaN, for which these fields are absent. For n-type doping of cubic GaN (c-GaN), Si has been used so far to achieve electron concentrations up to the $10^{19}\,cm^{-3}$ range [8–11]. It is reasonable to assume that employing Ge as a donor in c-GaN also leads to beneficial effects on the growth of highly doped layers as observed for hexagonal material and allows reaching electron concentrations of $10^{20}\,cm^{-3}$ and above. However, no experiments on the doping of c-GaN with Ge have been reported so far. In this report we present a first study on the incorporation of Ge into our c-GaN layers grown by plasma-assisted molecular beam epitaxy.

2 Experimental All c-GaN layers discussed in this work were grown by plasma-assisted molecular beam epitaxy in a Riber 32 system. Ga and Ge molecular beams were provided by effusion cells and an Oxford Applied Research HD25 radio frequency plasma source was used to generate activated nitrogen atoms. 10 μm thick 3C-SiC (001) layers, which are deposited on 500 μm Si (001), are used as substrates. All samples have been grown at a substrate temperature around 720 °C employing a Ga flux of $3.4 \times 10^{14}\,cm^{-2}\,s^{-1}$.

Samples with two different doping profiles have been fabricated. First, a series of samples each consisting of a nominally 600 nm thick Ge-doped c-GaN layer was grown. The Ge effusion cell temperature was varied between 600 and 1000 °C in steps of 100 °C to achieve doping levels varying over several orders of magnitude. The sample structure is sketched in Fig. 1a. For comparison, also a not intentionally doped 600 nm thick c-GaN layer was grown.

The second structure that has been grown is a multilayer stack sample containing several differently Ge-doped and

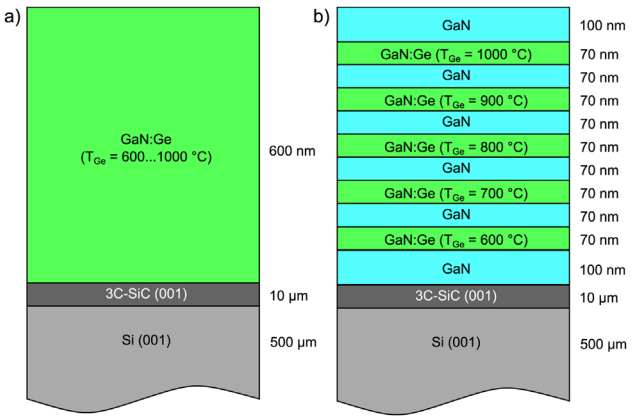

Figure 1 Structure of the grown Ge-doped c-GaN layers. (a) Series of samples consisting of a nominally 600 nm thick Ge-doped c-GaN layer grown with different Ge effusion cell temperatures. (b) Multilayer stack sample with doped c-GaN layers with various Ge concentrations embedded between undoped layers.

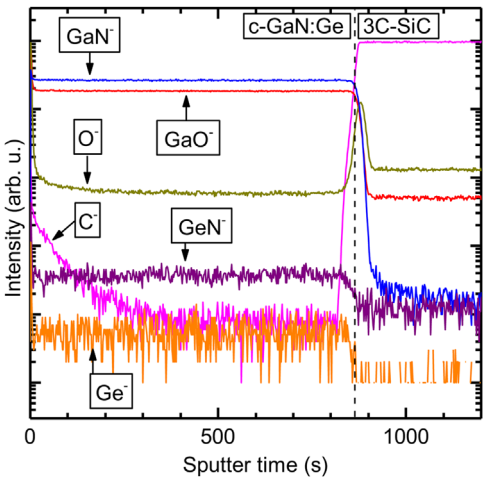

Figure 2 TOF-SIMS depth profile of the c-GaN layer grown with a Ge effusion cell temperature of $T_{Ge} = 800\,^{\circ}C$. The dashed vertical line at a sputter time of ~860 s indicates the transition from the c-GaN layer to the 3C-SiC substrate. The appearance of the Ge^- and GeN^- signals prove the incorporation of Ge into our c-GaN layers.

undoped layers (see Fig. 1b). First, a 100 nm thick undoped c-GaN layer was deposited. Subsequently doped and undoped layers with a thickness of 70 nm each were grown alternately. For each doped region the Ge cell temperature was increased by 100 °C, starting at 600 °C. On top of the last doped layer a 100 nm thick undoped GaN layer was deposited, eventually.

Time-of-flight secondary ion mass spectrometry (TOF-SIMS) was performed with an ION-TOF TOF-SIMS 5 to create a depth profile of the composition of our layers. A pulsed 15 keV-$^{69}Ga^+$ ion beam scanning a $(50 \times 50)\,\mu m^2$ area was used for analysing the sample. Depth profiling was done using a pulsed 1.0 keV-Cs^+ beam covering an area of $(300 \times 300)\,\mu m^2$. To prevent charging of the samples a pulsed electron shower was employed after each sputter step.

3 Results and discussion TOF-SIMS measurements on the samples of series (a) were performed to investigate the composition of the layers. Figure 2 shows the depth profile of the layer grown with a Ge effusion cell temperature of 800 °C. The sputter time is proportional to the depth the signals originate from. The profile can be divided into two parts as indicated by the dashed line. Up to a sputter time of approximately 860 s the signals originate from the c-GaN layer. The negative secondary ion signals originating from GaN^- and GaO^- run at a high intensity in this region. C^- and O^- ions are detected because of impurities in the layers. C and O are known to form acceptors and donors in c-GaN, respectively [8, 12]. An increase of the C concentration towards the sample surface can be observed. This behaviour is not apparent for all of the samples and should be investigated further. In the c-GaN layer, the O^- signal runs at a relatively high intensity. The unintentional n-type doping by O however can be disregarded, because the not intentionally doped sample shows p-type conductivity with a hole concentration around $10^{16}\,cm^{-3}$ while featuring the same O^- signal intensity. At the c-GaN/3C-SiC interface an increase of the O concentration can be observed. This is probably due to a residual oxidation of the substrate, although de-oxidation steps are performed.

The incorporation of Ge into our layers is proved by the appearance of signals that stem from Ge^- and GeN^- ions. Both signals proceed proportionally to each other, but the GeN^- signal features an approximately one order of magnitude higher sensitivity. The Ge-related signals remain constant within the c-GaN layer, so we conclude that homogeneous doping throughout the whole layer could be achieved. After a sputter time of about 860 s a significant change of the profile can be observed. The GaN^- and GaO^- signals decrease and the C^- signal increases strongly because the interface between the c-GaN layer and the 3C-SiC substrate is reached by the ion beams.

Due to the lack of a calibration sample, no absolute values for the Ge concentration could be extracted from the TOF-SIMS depth profiles. Instead, the ratio of the GeN^- intensity to the GaN^- intensity was calculated, which is proportional to the Ge concentration and allows to compare different TOF-SIMS experiments because the GaN^- signal intensity should be the same for all samples due to the identical N concentration. In Fig. 3 the values are plotted over the Ge effusion cell temperature. The vapour pressure curve of Ge [13] is plotted on a second scale, which is vertically shifted to fit to the TOF-SIMS data. The detection of Ge is limited by the noise level of the GeN^- signal which was determined from the not intentionally doped sample and is indicated by a dashed line in Fig. 3.

The amount of Ge found in the two samples with the lowest Ge concentration is significantly higher than it is expected from the vapour pressure curve. A Ge

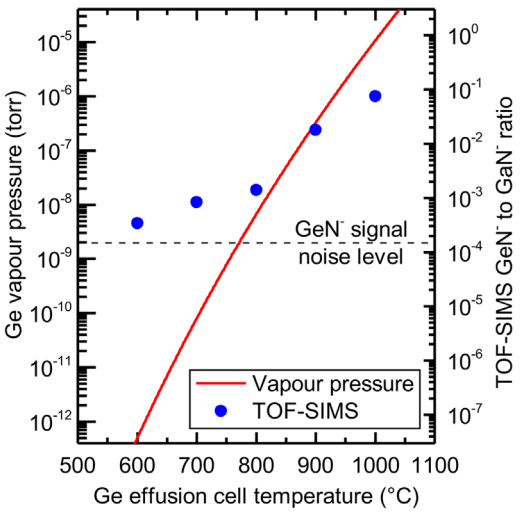

Figure 3 The ratios of the GeN^- to the GaN^- signals determined by TOF-SIMS measurements are plotted over the Ge effusion cell temperature. The noise level of the GeN^- signal, which limits the Ge detection, is indicated by a dashed line. The Ge vapour pressure curve is fitted to the TOF-SIMS data.

concentration in the order of 10^{14} and $10^{16}\,cm^{-3}$, respectively, is expected for these samples according to the vapour pressure curve. The Ge concentrations of more heavily doped samples are in good agreement to the trend of the vapour pressure curve, except for the sample with the highest Ge content ($T_{Ge} = 1000\,°C$). The calculated GeN^- to GaN^- intensity ratio lies clearly below the vapour pressure curve. We thus suppose that the incorporation efficiency of Ge drops at high Ge fluxes and the upper limit of incorporation is reached at this point. The electron concentration in this sample is $3.7 \times 10^{20}\,cm^{-3}$ (determined by Hall Effect measurements). For the second highest doped sample we measured an electron concentration of $8.7 \times 10^{19}\,cm^{-3}$. Due to the lack of absolute values for the Ge concentration, we could not determine the electrical activation of the incorporated Ge.

The nominal thickness of all layers is 600 nm. This value is based on an average growth speed of $133\,nm\,h^{-1}$ for undoped samples. The actual layer thickness was both measured by reflectometric interference spectroscopy and determined from TOF-SIMS measurements. From TOF-SIMS measurements the required sputter time until the interface between the c-GaN-layer and the 3C-SiC substrate is reached was taken to calculate the layer thickness. To calculate the sputter speed the layer thickness of the undoped sample measured by reflectometry was taken as a reference. The results are listed in Table 1. With increasing Ge effusion cell temperature, that is increasing Ge flux, the thickness of the layers decreases. The growth time of all samples was kept constant at 4.5 h, thus the growth speed is reduced due to the presence of Ge. At a Ge temperature of 1000 °C the growth speed is reduced by 40% compared to the undoped sample.

In Fig. 4 the TOF-SIMS depth profile of the sample comprising several differently doped layers is displayed. Doped and undoped layers can be distinguished by evaluating the Ge^- and GeN^- signals. Layers grown at higher Ge effusion cell temperatures feature higher Ge^- and GeN^- signal intensities.

The exact positions of the interfaces between doped and undoped layers are ambiguous because the Ge concentration changes gradually at the layer interfaces and does not drop to zero in undoped layers. We believe the observed Ge profile in the undoped layers has different origins for both interfaces of a layer. When sputtering the sample during TOF-SIMS analysis, some Ge atoms of doped layers are taken along into the undoped layers by recoil implantation, which explains the gradual decrease of the Ge concentration at the bottom boundaries of doped layers (seen in sputtering direction).

However, the decrease of Ge concentration is more gradual at the top boundaries of doped layers. We suppose that during growth of doped layers some excess Ge accumulates on the surface and is incorporated into the nominally undoped layers. This accumulation can be explained by means of the growth process. When growing undoped c-GaN layers, a Ga excess of exactly one monolayer is maintained by adjusting the Ga effusion cell and substrate temperature. Reflection high energy electron diffraction (RHEED) is used to monitor the Ga coverage of the surface. The presence of one excess monolayer of Ga has been proven to provide the best conditions for c-GaN growth [14]. During the growth of doped layers we also maintained an excess monolayer on the surface, which is now composed of Ga and Ge atoms. We assume that due to

Table 1 Thickness of the doped c-GaN-layers determined by reflectometric interference spectroscopy and TOF-SIMS. The layer thickness determined by TOF-SIMS is calculated from the time needed to sputter the c-GaN layer until the substrate is reached. The growth speed is calculated based on a growth time of 4.5 h, which was kept constant for all samples.

Ge temperature (°C)	– [a]	600	700	800	900	1000
layer thickness, reflectometry (nm)	612	588	556	543	460	363
layer thickness, TOF-SIMS (nm)	612	593	601	617	437	365
growth speed, reflectometry (nm/h)	136	131	124	121	102	81
growth speed, TOF-SIMS (nm/h)	136	132	134	137	97	81

[a]Undoped sample.

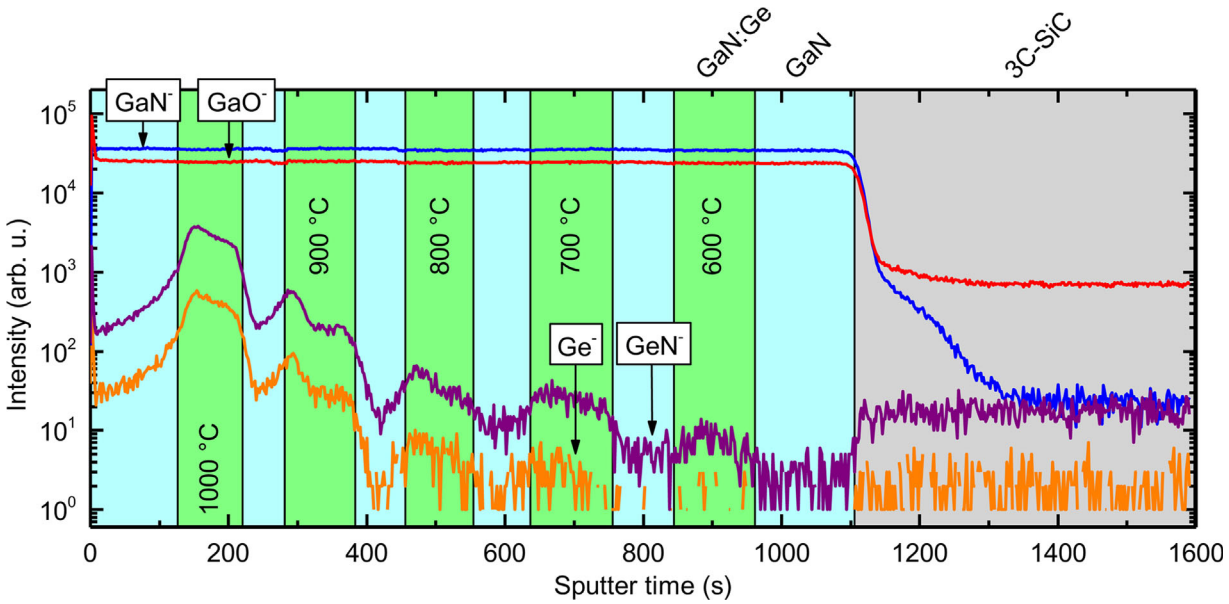

Figure 4 TOF-SIMS depth profile of the multilayer stack sample containing several differently Ge-doped and undoped layers. The doped and undoped layers and the substrate are highlighted in different shades. For the sake of clearness, the signals related to O and C impurities are discarded. The Ge effusion cell temperatures that were used for the doped layers are indicated in the diagram.

the higher dissociation energy of the Ge–Ge bond compared to the Ga–Ga bond (see Table 2) the evaporation of Ga from this excess layer is stronger than the evaporation of Ge. Therefore, an increasing amount of Ge can accumulate on the surface during growth.

The Ge excess could also explain the facts that the growth speed of highly doped layers decreases and that the Ge concentration in doped layers increases towards the sample surface. Impinging Ga atoms could be hindered by the Ge adlayer to reach the growth front, what reduces the growth speed. Additionally, considering the bond energies in Table 2, the Ge–N bond is formed more likely than the Ga–N bond. Thus, with an increasing amount of Ge on the surface more Ge is incorporated into the crystal, resulting in the increasing doping profile in the doped layers. The Ge concentration in the layer doped with a Ge effusion cell temperature of 900 °C shows a deviating behaviour. The concentration does not increase constantly towards the sample surface, but increases steeply near the upper interface of the layer. The reason for this behaviour is unclear; it is most likely caused by a fluctuation of the Ge flux. Similar structures grown by MOVPE, in contrast to our multilayer stack sample, exhibit constant doping profiles [19].

The 600 nm thick layers from series (a) exhibit a homogeneous doping profile, in contrast to sample (b). The exact reason of this difference is unclear. We assume that due to the significantly longer growth time the amount of Ge on the surface saturates and thus a constant doping density is achieved. Also, we cannot preclude that due to varying growth conditions Ge behaves differently on the sample surface. The effect that the two lowest doped samples contain a higher amount of Ge than it is expected from the vapour pressure curve could also be explained by the accumulation of Ge and the strong Ge–N bond.

To avoid the accumulation of Ge further optimization of growth needs to be done. The presence of a Ga excess monolayer has merely proven to provide the best growth conditions for undoped layers; one cannot necessarily assume that this is also the case for Ge-doped layers.

Table 2 Bond-dissociation energies ΔH for different bonds containing gallium and germanium.

bond	ΔH (kcal/mol)	Reference
Ge–N	61	[15]
	55	[16]
Ga–N	37.7	[17]
Ga–Ga	33	[18]
Ge–Ge	45	[15]
	65.5	[18]

4 Conclusions

Cubic GaN layers doped by germanium were grown by plasma-assisted molecular beam epitaxy. By varying the Ge effusion cell temperature, doping levels spanning a range of several orders of magnitude were realized. The incorporation of Ge was verified by time-of-flight secondary ion mass spectrometry (TOF-SIMS). Over a large temperature range of the Ge effusion cell the incorporated Ge concentrations follow the vapour pressure curve of Ge. For very high Ge fluxes a saturation of the Ge incorporation occurs; the highest electron concentration that was achieved is $3.7 \times 10^{20}\,\mathrm{cm}^{-3}$. This concentration is

about one order of magnitude higher than that reached by Si-doping. The thickness of the grown layers was determined by reflectometric interference spectroscopy and TOF-SIMS. A reduction of the growth rate was found when applying high Ge fluxes, which is ascribed to the accumulation of Ge on the sample surface during growth. A multilayer stack sample comprising several 70 nm thick layers with different Ge concentration separated by undoped interlayers was grown. The Ge accumulation during the growth of doped layers caused an unintentional doping of subsequently grown undoped layers. Also an increase of the Ge concentration within the doped layers was found. Doped layers with higher thickness however feature a homogeneous doping profile.

Acknowledgements The authors like to acknowledge financial support by the Deutsche Forschungsgemeinschaft (DFG) via the SFB/TRR 142.

References

[1] L. T. Romano, C. G. Van de Walle, B. S. Krusor, R. Lau, J. Ho, T. Schmidt, J. W. Ager, III, W. Götz, and R. S. Kern, Physica B **273–274**, 50 (1999).
[2] S. Fritze, A. Dadgar, H. Witte, M. Bügler, A. Rohrbeck, J. Bläsing, A. Hoffmann, and A. Krost, Appl. Phys. Lett. **100**, 122104 (2012).
[3] A. Dadgar, J. Bläsing, A. Diez, and A. Krost, Appl. Phys. Express **4**, 011001 (2011).
[4] R. Kirste, M. P. Hoffmann, E. Sachet, M. Bobea, Z. Bryan, I. Bryan, C. Nenstiel, A. Hoffmann, J.-P. Maria, R. Collazo, and Z. Sitar, Appl. Phys. Lett. **103**, 242107 (2013).
[5] P. R. Hageman, W. J. Schaff, J. Janinski, and Z. Liliental-Weber, J. Cryst. Growth **267**, 123 (2004).
[6] M. Wieneke, H. Witte, K. Lange, M. Feneberg, A. Dadgar, J. Bläsing, R. Goldhahn, and A. Krost, Appl. Phys. Lett. **103**, 012103 (2013).
[7] J. Schörmann, P. Hille, M. Schäfer, J. Müßener, P. Becker, P. J. Klar, M. Kleine-Boymann, M. Rohnke, M. de la Mata, J. Arbiol, D. M. Hofmann, J. Teubert, and M. Eickhoff, J. Appl. Phys. **114**, 103505 (2013).
[8] D. J. As, Defect Diffus. Forum **206–207**, 87 (2002).
[9] R. E. L. Powell, S. V. Novikov, C. T. Foxon, A. V. Akimov, and A. J. Kent, Phys. Status Solidi C **11**, 385 (2014).
[10] E. Martinez-Guerrero, B. Daudin, G. Feuillet, H. Mariette, Y. Genuist, S. Fanget, A. Philippe, C. Dubois, C. Bru-Chevallier, G. Guillot, P. Aboughe Nze, T. Chassagne, Y. Monteil, H. Gamez-Cuatzin, and J. Tardy, Mat. Sci. Eng. B **82**, 59 (2001).
[11] Z. Q. Li, H. Chen, H. F. Liu, L. Wan, M. H. Zhang, Q. Huang, J. M. Zhou, N. Yang, K. Tao, Y. J. Han, and Y. Luo, Appl. Phys. Lett **76**, 3765 (2000).
[12] C. G. Van de Walle and J. Neugebauer, J. Appl. Phys. **95**, 3851 (2004).
[13] O. Madelung, U. Rössler, and M. Schulz (eds.), Germanium (Ge), heats of fusion and sublimation, enthalpy and entropy, vapor pressure, in: Landolt-Börnstein, Group III, Vol. 41, Subvol. A1b (Springer-Verlag, Berlin, Heidelberg, 2002), Online Document 533, p. 1.
[14] J. Schörmann, S. Potthast, D. J. As, and K. Lischka, Appl. Phys. Lett. **90**, 041918 (2007).
[15] D. A. Johnson, Some Thermodynamic Aspects of Inorganic Chemistry (Cambridge University Press, Cambridge, 1976), p. 159.
[16] F. P. Pruchnik, Organometallic Chemistry of the Transition Elements (Springer, New York, 1990), p. 202.
[17] S. Porowski and I. Grzegory, in: Properties of Group III Nitrides, edited by J. H. Edgar (INSPEC, London, 1994), p. 76.
[18] J. A. Dean, Lange's Handbook of Chemistry, 15th edition (McGraw-Hill, New York, 1999), p. 4.45.
[19] C. Berger, A. Lesnik, T. Zettler, G. Schmidt, P. Veit, A. Dadgar, J. Bläsing, J. Christen, and A. Strittmatter, J. Cryst. Growth **440**, 6 (2016).